

Introducing Projective Transformations into Lunar Image Correspondence for Positioning Large Distance Rover

Chuankai Liu, Baofeng Wang, Xu Yang, Ping Miao, Geshi Tang, Kun Dai, Jia Wang, Xiaoxue Wang
and Xiangyan Guo

Abstract—Positioning rovers with a large distance is an important mission of the ground tele-operation center, which can decrease or eliminate the position errors accumulated in continuous measurement and multiple calculations, and facilitate the rover to arrive at faraway scientific probing targets. Currently, the most representative high-accuracy positioning methods are implemented with multi-camera photogrammetric model, which takes the homonymous point pairs extracted from images as constraint points of camera bundles to establish observation equations. The amount, spatial distribution and matching accuracy of homonymous point pairs will affect the effectiveness and accuracy of rover positioning. However, in the case of long-range moving, the images acquired by rover in two positions with a fairly big distance are difficult to match due to existence of large scale and rotation transformations, reflected view of the same scenery and different illumination conditions between acquired images, and a lot of outliers will be generated. In this paper, we introduce projective transformations, which are approximately calculated with imaging relations of two positions, to tackle the outlier elimination problem, and design an iterative algorithm to reduce the outliers and refine the positioning results simultaneously. With this method, the initial approximate positioning information of the rover can be utilized to constrain the range of each feature point projected to another image, and outliers are reduced gradually, preserving almost all the inliers. Finally, several experiments are conducted with lunar surface images acquired by Chang'E-3 rover, which witness the validity of the proposed method.

I. INTRODUCTION

DETERMINATION of its own position and orientation is very important to a lunar rover, which guarantees the rover reach the target to be probed and accomplish the probing tasks. Due to the limitation of rover on-board processing capacity, accurate localization is usually implemented by the ground tele-operation center. For example, in the China's ChangE-3 mission, positions of all navigation station that the "Yutu" rover reaches are calculated and estimated by the ground tele-operators. Different from positioning on the earth where a lot of priori knowledge on

This work was supported in part by the National Natural Science Foundation of China under Grant 61305137 and 61503383, in part by the Equipment Development Foundation under Grant 9140A04030114KG13 003.

C.K. Liu is with the Key Laboratory of Science and Technology on Aerospace Flight Dynamics, Beijing Aerospace Control Center, 100094, Beijing, China (corresponding author to provide phone: 8610-66361890; e-mail: ckliu2005@126.com).

B.F. Wang, is with the Key Laboratory of Science and Technology on Aerospace Flight Dynamics, Beijing Aerospace Control Center, 100094, Beijing, China.

X. Yang is with the Institute of Automation, Chinese Academy of Sciences, 100190, Beijing, China (e-mail: xu.yang@ia.ac.cn).

the environments exists and the GPS-like devices can be easily used to acquire accurate positions in a long-term travel, position determination of the lunar rover should depend on the very limited information acquired by the rover and transmitted to the ground tele-operation center. Especially in the case of long-range moving, the images transmitted to the ground may be acquired by rover in two positions with a fairly big distance, and there could exist large scale and rotation transformations, reflected view of the same scenery, and different illumination conditions between acquired images, which makes the image correspondence work very difficult. How to use these images, associated with some other remote sensing information, to accomplish accurate localization is a hard but very crucial task for long range exploration of the rover.

Currently, many researchers have proposed typical positioning models to solve the problem, mainly include spatial intersection [1, 2], visual odometry [3, 4] and bundle adjustment [5, 6]. These methods have been applied to lunar and mar exploration, successfully guiding rovers move in a long-distance range. Among these methods, localization based on bundle adjustment model can take ground control points, tie points, camera calibration parameters, and various distortion parameters into account to iteratively decrease the position error to a low level [6], consequently generating more precise results. In the condition that camera calibration parameters and various distortion parameters are known, how to exactly extract and recover control points and tie points from rover-acquired images becomes the key issue of rover localization.

Over the past few decades, there have been many concerns on vision-based localization of rovers in unstructured environments and major advances have occurred in guiding an extra-tellurian patrolling exploration. The most representative cases are the vision odometry systems installed in Spirit, Opportunity, and Curiosity Mars rovers [7, 8]. The system computes an update to the six-degree-of-freedom rover pose by finding features in a stereo image pair and tracking them from one frame to the next. In their method, an interest operator tuned for corner detection (e.g. Forstner or Harris) is applied to an image pair, and pixels with the highest interest values are selected. Each selected feature's 3D position is computed by stereo matching, which is done strictly along the epipolar line with only a few pixels of offset buffer above and below it. Similar works are also done by others [3, 4], which uses different methods in the stereo matching and meanwhile brings the rover motion-predict model into feature tracking. In the stereo matching, normalized correlation method is adopted to find the

corresponding location for each of selected features from the right image of the stereo. In the feature tracking, the prior knowledge of the approximate robot motion is used to constrain the search space, which improves the tracking efficiency.

Another typical example is the ExoMars Rover [9], which is produced by the European Space Agency (ESA) and aims to characterize in detail the Mars biological environment in preparation for future missions, including human exploration. In its vision-based localization, the Scale Invariant Feature Transform (SIFT) features are chosen as the visual landmarks to compute relative movement of the camera. When the rover moves around the Mars surface, many visual landmarks are observed from different angles, distances or under different illumination, and are automatically identified and tracked through SIFT-based matching algorithm. However, for the rover that moves station by station with a large distance, it is very difficult to get a robust correspondence for key points in the two images that have large scale and rotation transformations and very different illumination conditions, which requires new exploration on feature matching. Traditional appearance matching algorithms, like SIFT and its derived methods, often fail in handling the above situations. Some improved appearance matching algorithms, which take the affine transformation of images into account, such as affine SIFT, perform better than traditional ones in handling large-scale transformation problem, but they are still not able to obtain satisfactory results in tackling the above situations.

In this paper, we develop a novel matching method that first utilizes the imaging relation contained in the large-span moving of the rover to approximately compute the homography transformation between large-deformed images, and then takes transformed images as transitive ones to achieve precise matching. With this method, the inaccurate positioning information outputted by the internal navigation unit of rover can be utilized in the image matching, which reduces the probability of mistaken deletion when many outliers exist and improves the accuracy and stability of the rover positioning.

The rest parts of this paper are arranged as follows. In Section II, the framework of lunar rover localization is introduced and the bundle adjustment model is reformulated briefly. In section III, an iterative algorithm an iterative algorithm that gradually reduces the error-matched points and simultaneously refines the positions of the rover is proposed and presented in detail. Experiments to validate the above methods are given in Section IV, and finally conclude this paper.

II. LOCALIZATION FRAMEWORK OF LUNAR ROVER

In our previous work [10-12], we presented a localization framework for the lunar rover in a large-span moving mode, which utilized homonymous point pairs extracted from images to build bundle adjustment model, and also gave the nonlinear squared least algorithm to solve the model. In this section, we first introduce the localization framework and reformulate the adjustment model briefly, and then analyze how the amount, spatial distribution and matching errors of the homonymous points affect the correctness and accuracy

of the localization result. The localization framework is illustrated in Fig. 1.

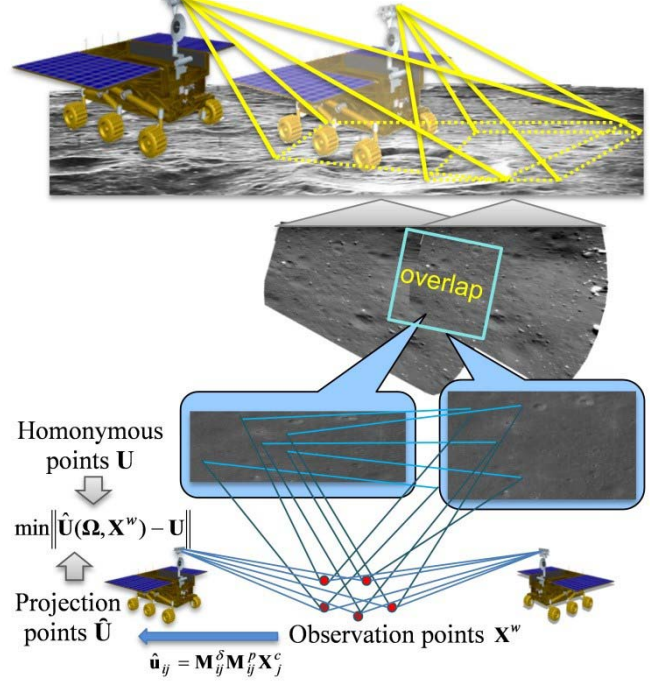


Fig. 1. Rover localization framework based on bundle adjustment model and image correspondence

The bundle adjustment model for rover localization is summarized as an optimization problem, which aims to minimizing the square of L_2 -norm of the deviations between the homonymous points extracted from images and the points calculated by perspective projection equations, defined as

$$(\hat{\Omega}, \hat{X}) = \arg \min_{\Omega, X^w} \sum_{i=1}^M \sum_{j=1}^N \|\hat{u}_{ij}(\Omega_i, X_j^w) - u_{ij}\|_2^2, \quad (1)$$

where $\hat{u}_{ij} = (\hat{u}_{ij}, \hat{v}_{ij}, 1)^T$ denotes the point projected to the i -th image plane by the j -th observation point, u_{ij} denotes the point extracted from the i -th image, $\Omega_i = (t_i, \theta_i)$ denote the translation and rotation of the i -th camera with respect to the world frame, and M and N denote the amount of cameras and observation points. \hat{u}_{ij} is calculated with the imaging model of perspective projection as

$$\hat{u}_{ij} = M_{ij}^{\delta} M_{ij}^p X_j^c = M_{ij}^{\delta} M_{ij}^p [R(\theta_i) | -R(\theta_i)t_i] X_j^w, \quad (2)$$

where $X_j^c = (X_j^c, Y_j^c, Z_j^c, 1)^T$ and $X_j^w = (X_j^w, Y_j^w, Z_j^w, 1)^T$ respectively denote the homogenous coordinate of the j -th surface point in the camera frame and the world frame, $M_{ij}^p \in \mathbf{R}^{3 \times 3}$ is the perspective transform matrix from j -th surface point to i -th image plane, and $M_{ij}^{\delta} \in \mathbf{R}^{3 \times 3}$ is the distortion transform matrix with respect to the coordinate of the projection point, written as

$$\mathbf{M}_{ij}^p = \frac{1}{z_j^c} \begin{bmatrix} f_i^u & 0 & u_i^0 \\ 0 & f_i^v & v_i^0 \\ z_j^c & 0 & 1 \end{bmatrix}, \mathbf{M}_{ij}^\delta = \begin{bmatrix} 1 & 0 & -\Delta u_{ij} \\ 0 & 1 & -\Delta v_{ij} \\ 0 & 0 & 1 \end{bmatrix},$$

where f_i^u and f_i^v denote the focal length in pixel resolution, and (u_0, v_0) is the coordinate of the image principle point, and Δu_{ij} and Δv_{ij} are the offset of the projection point due to radial distortion, decentering distortion and thin prism distortion.

The optimization problem of Equ. (1) can be linearized by Taylor series expansion of the nonlinear function $\hat{\mathbf{u}}_{ij}(\boldsymbol{\Omega}_i, \mathbf{X}_j^w)$, convert to a linear least square problem as

$$(\Delta \hat{\boldsymbol{\Omega}}, \Delta \hat{\mathbf{X}}) = \arg \min_{\Delta \boldsymbol{\Omega}, \Delta \mathbf{X}} \|\mathbf{J}(\Delta \boldsymbol{\Omega}, \Delta \mathbf{X}) \cdot \begin{bmatrix} \Delta \hat{\boldsymbol{\Omega}} \\ \Delta \hat{\mathbf{X}} \end{bmatrix} - \mathbf{b}\|_2^2, \quad (3)$$

where $\mathbf{J}(\Delta \boldsymbol{\Omega}, \Delta \mathbf{X}) \in \mathbf{R}^{2MN \times (6M+3N)}$ is the Jacobi matrix, and

$\mathbf{b} \in \mathbf{R}^{2MN \times 1}$ is the error vector, and they are defined as

$$\mathbf{J}(\Delta \boldsymbol{\Omega}, \Delta \mathbf{X}) = \partial \hat{\mathbf{u}} / \partial [\Delta \boldsymbol{\Omega}^T, \Delta \mathbf{X}^T] = [\partial \hat{\mathbf{u}}_{ij} / \partial (\Delta \boldsymbol{\Omega}_i, \Delta \mathbf{X}_j)],$$

$$\mathbf{b} = [\mathbf{b}_{ij}] = [\mathbf{u}_{ij} - \hat{\mathbf{u}}_{ij}(\boldsymbol{\Omega}_i^0, \mathbf{X}_j^0)].$$

Thus, the optimization problem of Equ. (1) can be solved by iteratively solving Equ. (3) and updating $\hat{\boldsymbol{\Omega}}$ and $\hat{\mathbf{X}}$ with $(\hat{\boldsymbol{\Omega}}, \hat{\mathbf{X}}) = (\boldsymbol{\Omega}, \mathbf{X}) + (\Delta \hat{\boldsymbol{\Omega}}, \Delta \hat{\mathbf{X}})$.

III. INTRODUCING PROJECTIVE TRANSFORMATION TO LUNAR IMAGE CORRESPONDENCE

A rover moving on the lunar surface always uses inertial navigation information to roughly estimate its position, which is completed before visual localization and usually considered an inaccurate input of visual localization. Furthermore, the position information is also capable of estimating an approximate projective transformation for images acquired by the rover in two different places, and the projective transformation can be utilized to determine the correctly matched points and reduce the probability of mistaken deletion when many outliers exist. In this section, we aim to find the homography transformation between the images acquired in different places based on the perspective projection transformation of Equ. (4) and evaluate the correctness of each matched point pair. Then, with correctly matched points, we refine the rover position and re-evaluate the point pairs until convergence. The calculation of approximate homography transformation and the interactive refinement of matched points and localization results are separately presented in two subsections.

A. Homography Transformation Calculation

Assume that the lunar rover stays at two different positions, and corresponding left-camera poses (in the world frame) are $\boldsymbol{\Omega}_1 = [\mathbf{t}_1^T \boldsymbol{\theta}_1^T]^T$ and $\boldsymbol{\Omega}_2 = [\mathbf{t}_2^T \boldsymbol{\theta}_2^T]^T$, respectively. From the Equ. (2) in subsection II, we have that

$$\hat{\mathbf{u}}'_{ij} = \hat{\mathbf{u}}_{ij} + \Delta \mathbf{u}_{ij} = \mathbf{u}_i^0 + \frac{1}{z_j^c} \mathbf{diag}(f_i^u, f_i^v, 1) [\mathbf{R}_i | -\mathbf{R}_i \mathbf{t}_i] \mathbf{X}_j^w, \quad (4)$$

where $\mathbf{u}_i^0 = [u_i^0 \ v_i^0 \ 0]^T$ is the coordinate of the image principle point, $\Delta \mathbf{u}_{ij} = [\Delta u_{ij} \ \Delta v_{ij} \ 0]^T$ is the distortion offset, $\mathbf{X}_j^w = [x_j^w, y_j^w, z_j^w, 1]^T$ is the homogenous coordinate of the lunar surface point in the world frame, $\mathbf{diag}(f_i^u, f_i^v, 1)$ denotes a diagonal matrix, $\mathbf{R}_i = [\mathbf{r}_{i1}^T \ \mathbf{r}_{i2}^T \ \mathbf{r}_{i3}^T]^T$ and $\mathbf{t}_i = [t_i^x, t_i^y, t_i^z]^T$ respectively denote the rotational matrix and transformation vector of the camera frame with respect to the world frame, $z_j^c = \mathbf{r}_{i3}^T \mathbf{X}_j^w$ is the z -coordinate of the lunar surface point in the camera frame.

Denote by I_1 and I_2 the left images acquired in the 1st and the 2nd positions, and suppose that the overlapped region is nearer to the 1st position than the 2nd position, which means that the resolution of the overlapped region in the image I_1 is higher than that in I_2 . We aim to find the homography transformation from the image I_1 to the image I_2 based on the projection relations of Equ. (6). However, since the coordinates of observation points in the world frame could not be uniquely determined from the image points of I_1 , we are not able to deduce an explicit expression for the homography transformation. In order to establish the approximate projection relationship from the image coordinate $\hat{\mathbf{u}}_{ij}$ to the world coordinate \mathbf{X}_j^w , we assume that the lunar surface is perpendicular to z -axis of the world frame and the lunar surface point \mathbf{X}_j^w lies on the plane $z^w = z_0$. Thus, we can solve the linear matrix equation of Equ. (6), and obtain that

$$\begin{aligned} x_j^w &= \frac{1}{b_y a_x - b_x a_y} [(b_y \mathbf{A} - a_y \mathbf{B}) \mathbf{t}_1^T - z_0 (b_y a_z - a_y b_z)], \\ y_j^w &= \frac{1}{a_y b_x - a_x b_y} [(b_x \mathbf{A} - a_x \mathbf{B}) \mathbf{t}_1^T - z_0 (b_x a_z - a_x b_z)], \\ z_{1j}^c &= \mathbf{r}_{13} [x_j^w, y_j^w, z_0]^T - \mathbf{r}_{13} \mathbf{t}_1^T, \end{aligned} \quad (5)$$

where $\mathbf{A} = [a_x, a_y, a_z]$, $\mathbf{B} = [b_x, b_y, b_z]$, and they are defined as

$$\mathbf{A} = [a_x, a_y, a_z] = f_1^u \mathbf{r}_{11} - (\hat{u}'_{1j} - u_1^0) \mathbf{r}_{13},$$

$$\mathbf{B} = [b_x, b_y, b_z] = f_1^v \mathbf{r}_{12} - (\hat{v}'_{1j} - v_1^0) \mathbf{r}_{13}.$$

Thus, the coordinate of the point projected by \mathbf{X}_j^w on the image I_2 is calculated as

$$\begin{aligned} \hat{\mathbf{u}}'_{2j} &= \mathbf{u}_2^0 + \frac{1}{z_{2j}^c} \mathbf{diag}(f_2^u, f_2^v, 1) [\mathbf{R}_2 | -\mathbf{R}_2 \mathbf{t}_2] \mathbf{X}_j^w, \\ \hat{\mathbf{u}}_{2j} &= \hat{\mathbf{u}}'_{2j} - \Delta \mathbf{u}_{2j}(\hat{\mathbf{u}}'_{2j}). \end{aligned} \quad (6)$$

According to Equ. (5) and (6), we can project the image I_1 to the image plane of I_2 , generating a new image I_1^p that has a similar scale with the image I_2 . Each point $\hat{\mathbf{u}}_{1j}^p$ on the image I_1^p is corresponded to one point $\hat{\mathbf{u}}_{2j}$ on the image I_2 , and can be mapped back to $\hat{\mathbf{u}}_{1j}$ on the image I_1 . Thus, the homography transformation matrix can be obtained by solving the following optimization problem

$$\mathbf{H} = \arg \min_{\mathbf{H}} \sum_{j=1}^n \|\mathbf{H}\hat{\mathbf{u}}_{1j} - \hat{\mathbf{u}}_{1j}^p\|_2^2 + \|\hat{\mathbf{u}}_{1j}^p - \hat{\mathbf{u}}_{2j}\|_2^2, \quad (7)$$

where $\hat{\mathbf{u}}_{1j}$ is randomly picked around the whole image I_1 , $\hat{\mathbf{u}}_{2j}$ is calculated by Equ. (6), $n \geq 4$, and $\mathbf{H} = [\mathbf{h}_1 \ \mathbf{h}_2 \ \mathbf{h}_3]$ can be estimated by minimizing algebraic distance [13, 14] as follows.

Denote by $\mathbf{h} = [\mathbf{h}_1^T \ \mathbf{h}_2^T \ \mathbf{h}_3^T]^T$ the 9-vector of the entries of \mathbf{H} , and the problem of Equ. (7) is formulated as

$$\mathbf{h} = \arg \min_{\mathbf{h}} \sum_{j=1}^n \|[\hat{\mathbf{u}}_{1j}^T \otimes \mathbf{G}(\hat{\mathbf{u}}_{2j})]\mathbf{h}\|_2^2, \quad (8)$$

where $\mathbf{G}(\hat{\mathbf{u}}_{2j})$ is a cross-product matrix, which has the property that $\mathbf{G}(\hat{\mathbf{u}}_{2j})\mathbf{u}_{1j} = \hat{\mathbf{u}}_{2j} \times \mathbf{u}_{1j}$ for any $\hat{\mathbf{u}}_{2j}$ and \mathbf{u}_{1j} , and \otimes is the Kronecker product between matrices, from which yields that $[\hat{\mathbf{u}}_{1j}^T \otimes \mathbf{G}(\hat{\mathbf{u}}_{2j})]\mathbf{h} = \mathbf{G}(\hat{\mathbf{u}}_{2j})\mathbf{H}\hat{\mathbf{u}}_{1j}$. Singular value decomposition (SVD) to the matrix $\hat{\mathbf{u}}_{1j}^T \otimes \mathbf{G}(\hat{\mathbf{u}}_{2j})$ can approximately compute the vector \mathbf{h} as the column of right matrix associated with the smallest singular value.

B. Interactive Refinement of Match and Localization

In this subsection, we will first introduce how to utilize the homography matrix to delete error-matches points (outliers), where inaccurate positioning information of the rover is taken as initial constraints. Then, an iterative algorithm called IRML (interactive refinement of Match and Localization) is proposed, which gradually refines the localization results with preserved point pairs and simultaneously reduce the outliers until convergence. Outlier elimination and iterative algorithm are presented in detail.

With the homography matrix \mathbf{H} known, the distance constraints for correctly matched points (inliers) is defined as

$$\delta_j = \|\mathbf{u}_{2j} - \mathbf{H}\mathbf{u}_{1j}\|_2 < \xi_j, \quad j = 1, \dots, N, \quad (9)$$

where \mathbf{u}_{1j} and \mathbf{u}_{2j} denote the matched points of two left images I_1 and I_2 , and ξ_j is calculated as follows.

$$\xi_j = \max_k \|\bar{\mathbf{u}}_{2j} - \bar{\mathbf{u}}_{2j}^k\|_2, \quad (10)$$

where $\bar{\mathbf{u}}_{2j}$ is the point projected by \mathbf{u}_{1j} on the image plane of I_2 associated with positions \mathbf{t}_1 and \mathbf{t}_2 , and $\bar{\mathbf{u}}_{2j}^k$ is the

point projected by \mathbf{u}_{1j} on the image plane of I_2 associated with \mathbf{t}_1 and $\mathbf{t}_2 \pm \eta \|\mathbf{t}_2 - \mathbf{t}_1\|$, where η is the prospective offset rate. η is initially determined by the precision of rough localization and gradually decreases in the iterative process,

$$\eta = \frac{\alpha \max_j \|\mathbf{u}_{2j} - \mathbf{H}\mathbf{u}_{1j}\|_2 + (1 - \alpha) \text{mean}_j \|\mathbf{u}_{2j} - \mathbf{H}\mathbf{u}_{1j}\|_2}{\max_j \xi_j / \eta_0}, \quad (11)$$

where α is weight coefficient, satisfying $0 < \alpha < 1$. Then $\bar{\mathbf{u}}_{2j}^k$ ($k = 1, \dots, 8$) is computed as

$$\bar{\mathbf{u}}_{2j}^k = \mathbf{u}_2^0 - \Delta \mathbf{u}_{2j} + \frac{1}{z_{2j}^c} \mathbf{diag}(f_2^u, f_2^v, 1) [\mathbf{R}_2 \ | \ -\mathbf{R}_2 \mathbf{t}_2^k] \mathbf{X}_j^w,$$

$$\mathbf{t}_2^k = \mathbf{t}_2 \pm \eta \|\mathbf{t}_2 - \mathbf{t}_1\|,$$

$$= (t_2^x \pm \eta \|t_2^x - t_1^x\|, t_2^y \pm \eta \|t_2^y - t_1^y\|, t_2^z \pm \eta \|t_2^z - t_1^z\|)^T.$$

Matched points not satisfying the distance constraints of Equ. (9) will be taken as outliers and be eliminated. Thus, we design an iterative algorithm to gradually reduce the outliers and simultaneously refine the positions of the rover. First, delete outliers not satisfying Equ. (9) from the matched point set. Second, and take the remaining point pairs to compute the Jacobi matrix \mathbf{J} and the rover positions. Then, update the homography matrix \mathbf{H} with Equ. (7), associated with the new rover position. The above process is repeated until convergence. The algorithm is detailed as follows.

Algorithm

Inputs

I_i : Left image of the i -th position.

I_i' : Right image of the i -th position.

η : Accuracy of positioning results, denoted with percentage of moving distance. Initially, we set $\eta = 0.1$.

Immediate variables

I_1^p : Projection of I_1 on I_2 .

\mathbf{H} : Homography transformation matrix from I_1 to I_2 .

ξ : Distance constraint to eliminate error matched

points.

U_i : The set of matched feature points of I_i .

U_i^p : The set of feature points projected by U_i .

U_i' : The set of matched feature points of I_i' .

δ_j : Distance between point of U_1^p and that of U_2 .

Output

\mathbf{t}_i : Position of left camera at the i -th station.

\mathbf{R}_i : Rotational matrix between the frame of left camera and the world frame at the i -th position.

Repeat

Step 1

Project: $I_1 \rightarrow I_1^p(I_2)$ with Equ. (5) and (6);

Select $\{\hat{\mathbf{u}}_{1i} \in I_1\}$ and $\{\hat{\mathbf{u}}_{1i}^p \in I_1^p\}$, $i = 1, \dots, m$, $m \geq 4$, satisfying $\hat{\mathbf{u}}_{1i} \leftrightarrow \hat{\mathbf{u}}_{1i}^p$, and calculate H and $\xi_j(\eta)$

with Equ. (7) and (10).

Step 2

Get $U_1^p = \{u_{1j}^p\}$ and $U_2 = \{u_{2j}\}, j=1, \dots, N$ from

I_1^p and I_2 by matching feature points;

Project: $U_1^p \rightarrow U_1$ by $u_{1j} = H^{-1}u_{1j}^p$.

Step 3

For $j=1$

If,

Delete u_{1j} and u_{2j} from U_1 and U_2 .

End If

End For

Update H , δ_j and η with Equ. (7), (9) and (11).

Step 4

Get U_1^r and U_2^r from I_1^r and I_2^r by stereo matching.

Step 5

Calculate t_2 and R_2 by solving localization model of Equ. (1) with U_1^* , U_2^* , U_1^r and U_2^r as inputs.



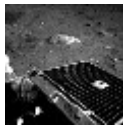
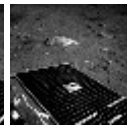

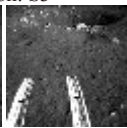
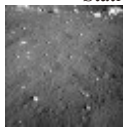
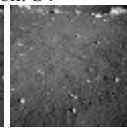
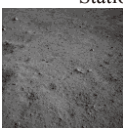
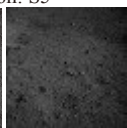

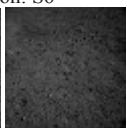
Until $\|\Delta t_2\| < \varepsilon_1$ or $\eta < \varepsilon_2$ or $\max \delta_j < \varepsilon_3$.

IV. EXPERIMENTS

In this section, we conduct experiments with lunar images that are acquired by ‘‘Yutu’’ rover in the Chang’E-3 mission. Totally two classes of experiments are presented, respectively show the improvement on selection of correctly matched points, and accuracy assurance of localization results in different calculations.

We choose three groups of images acquired at different adjacent stations to conduct rover localization experiments. The station number and corresponding left-camera images are shown in Table I.

TABLE I
THREE GROUPS OF IMAGES FROM DIFFERENT STATIONS

Group	Stations and Images			
	Station: S1		Station: S2	
1				
	left	right	left	right
	Station: S3		Station: S4	
2				
	left	right	left	right
	Station: S5		Station: S6	
3				
	left	right	left	right

Apply the IRML algorithm to the three groups of images, and iteratively calculate the localization results and reduce

error-matched points (outliers). Take the S1-S2 stations for example, each step of the iterative process is illustrated in Fig. 2, where $\xi_m = \max \xi_j$, $\delta = \text{mean } \delta_j$, N_{os} and N_{is} respectively denote the number of outliers and inliers. Note that in each step, the green lines connect matched points and white lines draw out the projection region of image I_1 on image I_2 .

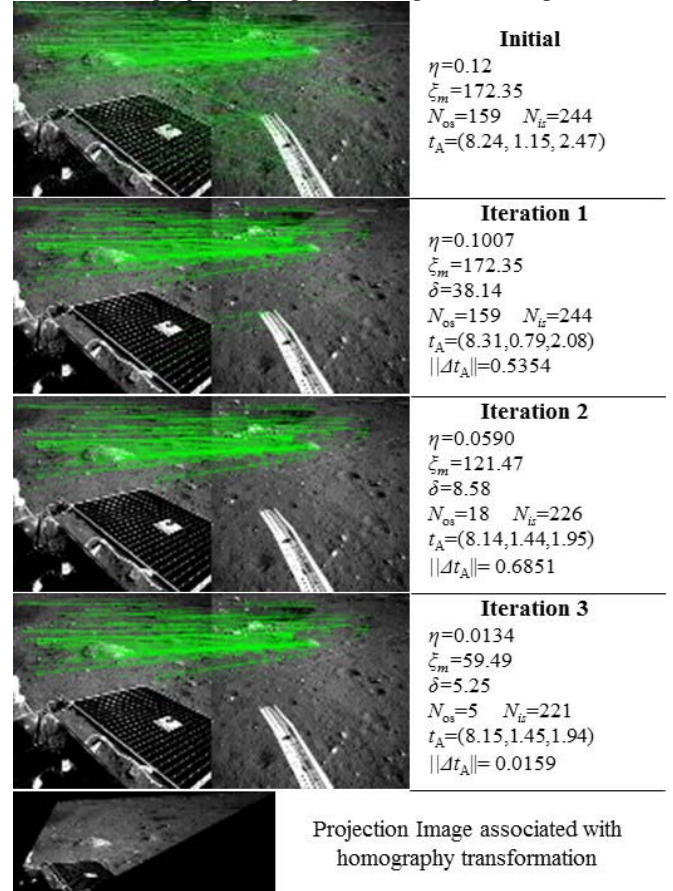


Fig. 2 Procedure for IRML algorithm applied to S1-S2 stations

From Fig. 2, we can see that the left images of S1-S2 stations initially contain nearly 40% outliers. As the offset rate η decreases, the outliers are gradually reduced until all the outliers are eliminated. Meanwhile, the pose of the rover at station S2 is refined until $\eta < 0.02$ and $\|\Delta t_2\| < 0.02$. Similarly, the main results of the other two groups are briefly presented in Table II, where the iterative times (ITs), number of preserved feature points, images with matched points and final positioning accuracy are contained.

TABLE II
THE MAIN RESULTS OF IRML ALGORITHM FOR S3-S4 AND S5-S6 STATIONS

stations	ITs	η	ξ_m	δ	N_{os}	N_{is}	$\ \Delta t_s\ $
S3-S4	4	0.0132	28.72	1.82	1267	458	0.0059
S5-S6	2	0.0134	32.81	2.40	979	387	0.0048

From Fig. 2 and Table II, it follows that, although there are many outliers in the matched points, even more most of matched points are outliers, the IRML algorithm can effectively handle the cases, and successfully separate inliers from matched points. The IRML algorithm can converge

within several steps, and the localization results are iteratively refined. In order to demonstrate the ability of IRML algorithm in assuring accuracy of localization results, we repeated four times of calculations for each pair of stations, and get the position results in Table III.

TABLE III
THE FINAL POSITION RESULTS OF IRML ALGORITHM REPEATING 4 TIMES

Times	Positioning Results		
	S1-S2	S3-S4	S5-S6
1	(8.147,1.449,1.942)	(6.172,0.122,1.989)	(0.663,-4.934,-0.377)
2	(8.155,1.446,1.945)	(6.190,0.129,1.992)	(0.670,-4.937,-0.376)
3	(8.136,1.452,2.007)	(6.161,0.136,1.983)	(0.668,-4.932,-0.375)
4	(8.149,1.438,1.972)	(6.159,0.121,1.935)	(0.668,-4.936,-0.372)
Δ_{max}	0.0107	0.0418	0.0048
$\Delta_{max}/\Delta t$	0.13%	0.65%	0.11%
$\Delta_{max}=\max_i\ (t_1+t_2+t_3+t_4)/4-t_i\ _2$, Δt : distance between stations			

V. CONCLUSION

This paper presents a method of localizing the lunar rover within local coordinate system using lunar surface images acquired by rover at two adjacent positions. The method is comprised of two main parts. One is constructing pose determination model for the rover and solving the model by minimizing the errors between the image points and the points projected from lunar surface to the image plane. The other is an iterative algorithm on the interactive refinement of matched points and localization result.

Since the pose determination model is the basis of rover localization, we first consider the specificity contained in the large-distance traverse of the rover, and derive a general model which integrates the rover transition, camera calibration, matched images points, and conversion between different frames together. From the deduction of the model, it is concluded that the accuracy of the rover pose is mainly influenced by the matching results of feature points extracted from the image pairs. Especially when the extracted feature points are very few, the pixel offset of feature matching will greatly influence the localization results. However, in the large-distance traverse of the rover, images acquired in two adjacent positions are very different in scale, rotation and illumination conditions, and this makes accurate matching very difficult.

In order to tackle the above problem, an iterative localization algorithm is proposed, which gradually reduce the outliers and simultaneously refines the localization results with preserved point pairs until convergence. Based on this method, we conduct two classes of experiments. One is to validate the efficiency of the novel matched method in selecting correctly matched points from a point set with many outliers included, and the other is to demonstrate the accuracy assurance of localization results after emerging the new matching method. Although the method of this paper performs better than that shown in Chang'E-3 mission, there are still some unpleasant aspects needing consideration in our future works, such as how to use the structural information to improve the matching performance. Also, some very interesting problems, such as matching two images acquired in reflected views, need further investigation and more attentions in our future works.

REFERENCES

- [1] Y. Huang, X.G. Hu, P.J. Li, J.F. Cao, D.R. Jiang, W.M. Zheng and M. Fan, Precise Positioning of Chang'E-3 Lunar Lander Using a Kinematic Statistical Method, Chinese Science Bulletin, 2012, 57(35): 4545-4551.
- [2] K. Di, A Review of Spirit and Opportunity Rover Localization Methods, Spacecraft Engineering, 2009, 18(5): 1-5.
- [3] C.F. Olson, L.H. Matthies, M. Shoppers and M. Maimone, Robust Stereo Ego-motion for Long Distance Navigation, IEEE Computer Society Conference on Computer Vision and Pattern Recognition, 2000, 2: 453-458.
- [4] C.F. Olson, L.H. Matthies, M. Shoppers and M. Maimone, Rover navigation using stereo egomotion, Robotics and Autonomous Systems, 2003, 43(4): 215-229.
- [5] R. Li, S.W. Squyres, R.E. Arvidson, et al, Initial results of rover localization and topographic mapping for the 2003 Mars exploration rover mission, Photogrammetric Engineering and Remote Sensing, Special issue on Mapping Mars, 2005, 71(10): 1129-1142.
- [6] K. Di, F. Xu, J. Wang et al, Photogrammetric processing of rover imager y of the 2003 Mars Exploration rover mission, I SPRS Journal of Photogrammetry and Remote Sensing, 2008, 63: 181-201.
- [7] Mark Maimone, Yang Cheng, and Larry Matthies, Two Years of Visual Odometry on the Mars Exploration Rovers, Journal of Field Robotics, vol. 24, no. 3, pp. 169-186, 2007.
- [8] Yang Cheng, Mark Maimone, and Larry Matthies, Visual Odometry on the Mars Exploration Rovers, IEEE Conference on Systems, Man and Cybernetics, 2005.
- [9] S. Se, T. Barfoot and P. Jasiobedzki, Visual Motion Estimation and Terrain Modelling for Planetary Rovers, The 8th International Symposium on Artificial Intelligence, Robotics and Automation in Space, ESA SP-603, 2005.
- [10] C.K. Liu, B.F. Wang, J.S. Shen, G.S. Tang et al., A Positioning Method of Chang'E-3 Rover in Large-span States Based on Cylindrical Projection of Images, Proceeding of the 11th World Congress on Intelligent Control and Automation, 2014, 2475-2480.
- [11] C.K. Liu, B.F. Wang, G.S. Tang, et al., Positioning Technology with Multi-source Information Integrated in the Chang'E-3 Lunar Landing and Exploration, International Astronautical Congress, 2014.
- [12] C.K. Liu, B.F. Wang, J.H. Su, et al., A Novel Matching Method of Large Deformed Images for Localizing Lunar Rovers with Large Distance, International Astronautical Congress, 2015.
- [13] R.I. Hartley and A.Ziserman, Multiple View Geometry in Computer Vision, Cambridge University, Cambridge, 2nd edition, 2003.
- [14] M. Sonka, V. Hlavac and R. Boyle, Image Processing, Analysis and Machine Vision, CL-Engineering, 3rd edition, 2008.